1521-009X/44/10/1720–1730$25.00
Drug Metabolism and Disposition
http://dx.doi.org/10.1124/dmd.116.071076
Drug Metab Dispos 44:1720–1730, October 2016

Perspective

Evaluation of CYP2B6 Induction and Prediction of Clinical Drug–Drug Interactions: Considerations from the IQ Consortium Induction Working Group—An Industry Perspective

Odette A. Fahmi, Mohamad Shebley, Jairam Palamanda, Michael W. Sinz, Diane Ramsden, Heidi J. Einolf, Liangfu Chen, and and Hongbing Wang

Pfizer Inc., Groton, Connecticut (O.A.F.); AbbVie Inc., North Chicago, Illinois (M.S.); Merck Research Laboratories, Rahway, New Jersey (J.P.); Bristol-Myers Squibb, Wallingford, Connecticut (M.W.S.); Boehringer Ingelheim, Ridgefield, Connecticut (D.R.); Novartis, East Hanover, New Jersey (H.J.E.); GlaxoSmithKline, King of Prussia, Pennsylvania (L.C.); and University of Maryland School of Pharmacy, Baltimore, Maryland (H.W.)

Received April 20, 2016; accepted July 14, 2016

ABSTRACT

Drug–drug interactions (DDIs) due to CYP2B6 induction have recently gained prominence and clinical induction risk assessment is recommended by regulatory agencies. This work aimed to evaluate the potency of CYP2B6 versus CYP3A4 induction in vitro and from clinical studies and to assess the predictability of efavirenz versus bupropion as clinical probe substrates of CYP2B6 induction. The analysis indicates that the magnitude of CYP3A4 induction was higher than CYP2B6 both in vitro and in vivo. The magnitude of DDIs caused by induction could not be predicted for bupropion with static or dynamic models. On the other hand, the relative induction score, net effect, and physiologically based pharmacokinetics SimCYP models using efavirenz resulted in improved DDI predictions. Although bupropion and efavirenz have been used and are recommended by regulatory agencies as clinical CYP2B6 probe substrates for DDI studies, CYP3A4 contributes to the metabolism of both probes and is induced by all reference CYP2B6 inducers. Therefore, caution must be taken when interpreting clinical induction results because of the lack of selectivity of these probes. Although in vitro–in vivo extrapolation for efavirenz performed better than bupropion, interpretation of the clinical change in exposure is confounded by the coinduction of CYP2B6 and CYP3A4, as well as the increased contribution of CYP3A4 to efavirenz metabolism under induced conditions. Current methods and probe substrates preclude accurate prediction of CYP2B6 induction. Identification of a sensitive and selective clinical substrate for CYP2B6 (fraction metabolized > 0.9) is needed to improve in vitro–in vivo extrapolation for characterizing the potential for CYP2B6-mediated DDIs. Alternative strategies and a framework for evaluating the CYP2B6 induction risk are proposed.

Introduction

Given the importance of drug–drug interactions (DDIs) in the overall clinical safety profile of medications, the U.S. Food and Drug Administration (FDA), the European Medicines Agency (EMA), and the Japanese Ministry of Health, Labour and Welfare each provided guidance documents to industry for evaluating drug interactions, which also recommend procedures for predicting DDIs (http://www.fda.gov/downloads/drugs/guidancecomplianceregulatoryinformation/guidances/ucm292362; http://www.ema.europa.eu/docs/en_GB/document_library/Scientific_guideline/2012/07/WC500129606). Analogous to the regulatory guidance, several groups have published articles from an industry perspective on how best to predict DDIs caused by inhibition and induction of drug-metabolizing enzymes with a focus on CYP3A4 (Fahmi and Ripp, 2010; Einolf et al., 2014; Vieira et al., 2014). Throughout the regulatory guidance, DDIs related to cytochrome P450 (P450) interactions are analyzed and interpreted in a similar fashion with no distinction between P450 isoforms. However, in the area of enzyme induction and prediction of DDIs, there is a need for understanding whether the predictability of current data analysis methods and interpretation using these methods is similar across P450 enzymes. Therefore, following on previously published literature on CYP3A4-mediated enzyme induction (Fahmi et al., 2008b, 2009; Einolf et al., 2014), an assessment of data analysis methods to predict DDIs caused by enzyme induction of CYP2B6 would be of value. To identify the utility of CYP2B6 in vitro induction data, the International

dx.doi.org/10.1124/dmd.116.071076.
This article has supplemental material available at dmd.aspetjournals.org.

ABBREVIATIONS: AUC, area under the concentration curve; AUCR, area under the concentration curve ratio with and without precipitant drug; DDI, drug–drug interaction; DMSO, dimethylsulfoxide; EMA, European Medicines Agency; E_{max}, maximum fold increase over vehicle control; FDA, Food and Drug Administration; f_m, fraction metabolized; GMFE, geometric mean fold error; IQ, International Consortium for Innovation and Quality in Pharmaceutical Development; IVIVE, in vitro–in vivo extrapolation; MS/MS, tandem mass spectrometry; NME, new molecular entity; P450, cytochrome P450; PBPK, physiologically based pharmacokinetics; PCPAH, *trans*-2-phenylcyclopropylamine hydrochloride; PCR, polymerase chain reaction; RIS, relative induction score; TDI, time-dependent inhibition; UGT, uridine 5′-diphosphoglucuronosyltransferase.

Consortium for Innovation and Quality in Pharmaceutical Development (IQ Consortium) launched a CYP2B6 Induction Working Group. The IQ Consortium is an organization of pharmaceutical and biotechnology companies providing a forum to address issues for the biopharmaceutical industry. This white paper presents observations from the IQ Consortium working group and provides an initial framework on issues and approaches to consider when evaluating the induction of CYP2B6.

CYP2B6 is one of the highly inducible and polymorphic P450 isoforms expressed predominantly in the human liver (Zanger et al., 2007; Wang and Tompkins, 2008). To date, large variations in CYP2B6 due to induction and polymorphisms have been demonstrated in humans. Interindividual differences in hepatic CYP2B6 expression levels and activity have been reported to vary up to several hundredfold (Ekins et al., 1998; Faucette et al., 2000). As such, interindividual differences in CYP2B6 catalytic capacity may result in variable systemic exposure to drugs that are metabolized by CYP2B6, including the antineoplastic drugs cyclophosphamide and ifosfamide (Roy et al., 1999), the antiretrovirals nevirapine and efavirenz (Ward et al., 2003), the anesthetics propofol and ketamine (Court et al., 2001), and the antiparkinsonian drug selegiline (Hidestrand et al., 2001). Although CYP2B6 does not play a major role in the metabolism (elimination) of many marketed drugs, efavirenz and bupropion are two drugs described in the literature and in regulatory guidance documents as sensitive probe substrates to date for the assessment of CYP2B6 enzyme activity in vitro and in vivo.

During the past 10 years, important advances have been made in our understanding of the mechanisms that regulate induction of hepatic CYP2B6. The constitutive androstane receptor (NR1I3) has been identified as the primary mediator for drug-induced expression of CYP2B6, whereas the pregnane X receptor (RN1I2) is predominantly responsible for CYP3A4 induction (Lehmann et al., 1998; Sueyoshi et al., 1999). Nevertheless, these two closely related nuclear receptors can recognize and bind to response elements located in both CYP2B6 and CYP3A4 promoters (Xie et al., 2000; Faucette et al., 2007). The crosstalk between the constitutive androstane receptor and pregnane X receptor (Zanger et al., 2007) results in shared mechanisms of transcriptional regulation of CYP2B6 and CYP3A4 and many known CYP2B6 inducers also increase the expression of CYP3A4 (Fahmi et al., 2010; Tolson and Wang, 2010).

It is evident that drug-induced expression of CYP2B6 contributes to the highly variable CYP2B6 expression in the human liver. However, the majority of data evaluating CYP2B6 induction have been obtained from sparse in vitro cell-based experimental systems and clinical DDI results. Reliable and predictive in vitro–in vivo extrapolation (IVIVE) models, combining more comprehensive clinical data sets with extensive in vitro experimental results, would be highly desirable. To that end, this article describes assessments of the potency of CYP2B6 versus CYP3A4 induction in vitro and from clinical studies, the reliability of efavirenz versus bupropion as clinical probe substrates for CYP2B6 induction, and the performance of various data analysis methods [the FDA basic R3 model, the relative induction score (RIS), the net effect model, and the SimCYP physiologically based pharmacokinetics (PBPK) model] to predict the clinical outcome of CYP2B6 enzyme induction–mediated DDIs.

Materials and Methods

Reagents. Bupropion, cimetidine, carbamazepine, efavirenz, indinavir, nelfinavir, itraconazole, nifedipine, nevirapine, phenobarbital, phenytoin, rifampin, ritonavir, erythromycin, ticlopidine, *trans*-2-phenylcyclopropylamine hydrochloride (PCPAH), telmisartan, β-glucuronidase, glucose 6-phosphate, NADPH, and saquinavir were purchased from Sigma-Aldrich (St. Louis, MO).

^{14}C-Efavirenz was purchased from Moravak Biochemical (Brea, CA). Efavirenz metabolites were purchased from Toronto Research Chemicals (Toronto, ON, Canada). HepatoPac plates were purchased from Ascendance Biotechnology Inc. (formerly Hepregen, Medford, MA).

The RNeasy Mini Kit was from Qiagen (Valencia, CA) and the cDNA Reverse Transcription Kit was obtained from Applied Biosystems (Foster City, CA). Pooled human liver microsomes (150-donor pool) were purchased from Gentest/Corning Discovery Labware (Woburn, MA). All cell culture reagents were purchased from Life Technologies (Carlsbad, CA) unless otherwise noted.

Culture of Cryopreserved Human Hepatocytes. Various lots of human cryopreserved hepatocytes (Supplemental Table 4) were obtained from different commercial vendors, including CellzDirect (Durham, NC), Bioreclamations In Vitro Technologies (Baltimore, MD), and XenoTech LLC, (Kansas City, KS). As detailed in previous publications (Fahmi et al., 2010; Ramsden et al., 2015), cryopreserved human hepatocytes (Supplemental Tables 1 and 4) were thawed in hepatocyte thawing medium and were seeded in collagen I–coated 24- or 96-well plates at cell densities of 0.5 to 1 $\times$ 10^6 viable cells per well in hepatocyte plating medium. Viability, as determined by trypan blue exclusion or other methods, was 85% or better when cells were plated. The cells were initially maintained at 37°C in a humidified incubator with 95% atmospheric air and 5% CO_2 overnight in hepatocyte incubation media. After overnight incubation, the cells were treated with various compounds. Compounds were dissolved in dimethylsulfoxide (DMSO) and added to the culture medium at various concentrations (final DMSO concentration, 0.1%). After 2 days of daily treatment, the medium was removed and the cells were washed with saline. The cells were lysed in lysis buffer and prepared for RNA isolation. Cell viability was assessed by visual inspection of the monolayer, checking for confluence and morphology. Different companies used different plating conditions and a representation of the conditions is shown in Supplemental Table 1.

Real-Time Polymerase Chain Reaction and Quantification of CYP3A4 and CYP2B6 mRNA. After the isolation of RNA using commercially available kits, cDNA was synthesized using standard polymerase chain reaction (PCR) protocols. CYP3A4, CYP2B6, and an endogenous probe (e.g., glyceraldehyde-3-phosphate dehydrogenase mRNA levels) were quantified by real-time PCR. The gene-specific primer/probe sets were obtained from Applied Biosystems and real-time PCR was performed using CYP3A4, CYP2B6, and the endogenous control target cDNAs. The relative quantity of the target cDNA compared with that of the control glyceraldehyde-3-phosphate dehydrogenase was determined by the $\Delta\Delta$ threshold cycle method (Applied Biosystems User Bulletin 2). Threshold cycle values > 32 were excluded from the analysis. Relative quantification measured the change in mRNA expression in a test sample relative to that in a vehicle control sample (0.1% DMSO).

Determination of E_{max} and EC_{50} Values. The in vitro induction mRNA data were fitted using the following sigmoid three-parameter equation:

$$\text{Induction response} = E\text{max}/(1 + \text{Exp}(-([\text{I}] - \text{EC50})/\text{slope}))$$

Commercially available software such as SigmaPlot (Systat Software, San Jose, CA) or GraphPad Prism (GraphPad Software Inc., La Jolla, CA) was used to calculate E_{max} (maximum fold increase over vehicle control) and EC_{50} (the in vitro concentration of inducer that produced half the maximum induction) values.

Kinetic parameters (EC_{50} and/or E_{max}) estimated from a particular donor that showed a high standard error (>100% of the estimated value) were excluded from the analysis. Mean values of the pooled data gathered from different companies were used in the analysis (Table 3; Supplemental Tables 2 and 3).

Efavirenz Metabolism Using the Induced Long-Term HepatoPac Model. HepatoPac long-term hepatocytes were purchased from Ascendance Biotechnology Inc. HepatoPac products ("hepatocytes") are micropatterned to create proprietary patterns of hepatocyte "islands" surrounded by supportive stromal cells. This technology replicates the physiologic microenvironment of the liver and allows the hepatocytes to exhibit normal metabolic activity for over 4 weeks.

Human hepatocytes were induced with [^{14}C]-efavirenz (final concentration of 10 μM) in a 24- or 96-well plate format for 96–120 hours, using four hepatocyte donors (Table 4; Supplemental Table 4). Induced human HepatoPac plates were then further incubated with and without inducers for 72 hours (10 μM rifampin,

10 μM efavirenz, or 100 μM carbamazepine) or inhibitors (50 μM erythromycin, 10 μM ticlopidine, 10 μM telmisartan, or 10 μM PCPAH) with a total volume of 400 μl per well. At 24 hours, 96 hours, and 120 hours, 800 μl reaction termination solution (99.9% acetonitrile and 0.1% acetic acid) was added to the wells and the cells were scraped from the bottom of the well. These samples were then transferred to 2-ml Fisher low nonspecific binding vials (Fisher Scientific, Pittsburg PA). Removal of cell monolayers was confirmed microscopically. After centrifugation, the supernatants were analyzed by liquid chromatography/radio chromatography/tandem mass spectrometry (MS/MS) for quantitative metabolite identification. Samples of [^{14}C]-efavirenz were analyzed by an ultra-performance liquid chromatography LTQ Orbitrap (Thermo Scientific, San Jose, CA) coupled with a flow scintillation radiomatic detector (PerkinElmer, Waltham, MA). Metabolite separation was achieved using a Gemini C_{18} column (3 μm, 150 × 4.6 mm; Phenomenex, Torrance, CA) with gradient elution. The mobile phase consisted of 95:5 (v/v) water/acetonitrile and 95:5 (v/v) acetonitrile/water. Both mobile phases contained 0.1% acetic acid. The samples generated from incubation of ^{14}C-efavirenz with HepatoPac were analyzed by an LTQ Orbitrap for metabolite identification using high-resolution, full-scan mass spectometry aligned with radiometric chromatograms. The MS/MS scans (at high or unit resolution) were conducted to identify structures of metabolites. The peak areas of metabolites and parent generated from the radiometric chromatograms and their relative exposures were calculated as the percentage of the total drug-related exposure. Where possible, confirmation of metabolite structures was performed using authentic standards and by deconjugation with glucuronidase for the glucuronide conjugates.

Determination of k_{obs}, k_{inact}, and K_I Values for CYP2B6 and CYP3A4. An IC_{50} shift assay for CYP2B6 was first conducted as a screen for identifying potential for time-dependent inhibition (TDI) (data not shown) as previously reported (Bjornsson et al., 2003). For select compounds (IC_{50} shift of > 1.5), definitive kinetic parameters K_I and k_{inact} were obtained. In vitro kinetic parameters for time-dependent inactivation of CYP2B6 or CYP3A4 in human liver microsomes were determined for each compound by preincubating pooled human liver microsomes (typically 0.5 or 1 mg protein/ml) with various concentrations of the test compounds in 100 mM potassium phosphate buffer (pH 7.4) containing $MgCl_2$ (5 mM) and NADPH for an incubation period ranging from 0 to 30 minutes. Aliquots of the preincubation mixture were removed at various time points and diluted 20-fold with the same buffer containing bupropion or midazolam at V_{max} concentrations and NADPH. The incubation was continued for an additional 6 minutes to monitor the extent of bupropion or midazolam hydroxylation using liquid chromatography–MS/MS. The first-order rate constants (k_{obs}) for inactivation at various concentrations were calculated from the negative slope of the lines by linear regression analysis of the natural logarithm of the remaining activity as a function of time. The k_{inact} and K_I (concentration of the inhibitor that produces half maximal rate of inactivation) values were calculated (Table 3) by nonlinear regression analysis as follows: $k_{obs} = k_{inact} \times [I]/(K_I + [I])$ (Einolf et al., 2014).

Data Collection of the Clinical Drug Interaction Studies. CYP2B6 in vivo DDI data used in this analysis were gathered from the University of Washington database. The compiled clinical data contained 14 and 16 clinical studies using bupropion and efavirenz as the substrate, respectively (Tables 1 and 2).

Net Effect Model. The previously reported equation for the combined mathematical model was used in this analysis with some modifications (Fahmi et al., 2008b). Since CYP2B6 is not known to be expressed in the intestine, only the liver term was used, as shown below. In addition, the TDI term was eliminated from the equation since there was no CYP2B6 TDI observed in vitro with the selected test compounds in this study. The net effect equation is expressed as the ratio of the area under the concentration-time curve in the presence (AUC'_{po}) and absence (AUC_{po}) of a pharmacokinetic DDI as follows:

$$\frac{AUC'_{po}}{AUC_{po}} = \left(\frac{1}{[B \times C] \times f_m + (1 - f_m)}\right)$$

B is the term for induction in the liver as follows:

$$B = 1 + \frac{d \bullet E_{max} \bullet [I]_H}{[I]_H + EC_{50,I}}$$

C is the term for reversible inhibition in the liver as follows:

$$C = \frac{1}{1 + \frac{[I]_H}{K_i}}$$

$[I]_H$ represents concentrations of inducer relevant for the liver utilizing the unbound systemic C_{max}. The scaling factors (d) were 0.50 and 1 with efavirenz and bupropion, respectively. The fraction metabolized (f_m) CYP2B6 values used in the net effect static model were 0.64 and 0.50, consistent with SimCYP default values for efavirenz and bupropion, respectively. The bias of the different prediction approaches was assessed by calculation of the geometric mean folds error (GMFE) of the data, as previously described (Fahmi et al., 2009).

PBPK Modeling. The mean E_{max} and EC_{50} values for CYP2B6 and CYP3A4 (calculated from all of the mRNA induction assessments for each perpetrator) as well as the inhibition parameter K_i, K_I, and k_{inact} values were used in the PBPK modeling. Simulations for bupropion and efavirenz as victim drugs (shown in Tables 5 and 6) were assessed using SimCYP versions 14.1 and 15.1, respectively, without normalization of the in vitro data. However, we fully characterized the CYP2B6 in vitro induction potential of the inducers (Supplemental Table 2). Unlike the extensive wealth of clinical data described for CYP3A4 induction by rifampin, CYP2B6 clinically validated data are lacking to attempt normalization. The victim bupropion compound default file was available in SimCYP version 14.1, and the efavirenz compound default file used SimCYP version 15.1. The efavirenz SimCYP file was updated with the newly generated in vitro parameters (K_i, K_I, k_{inact}, EC_{50}, and E_{max}) for both CYP3A4 and CYP2B6 (Table 3). Perpetrators with available model files within the SimCYP compound library were updated with newly generated CYP2B6 and CYP3A4 induction data (without normalization to rifampin; Ke et al., 2016) and/or any missing inhibition/inactivation kinetic parameters, as shown in Table 3. Perpetrator compounds that had to be built were validated using published clinical pharmacokinetic information to ensure that the models reasonably recapitulated day 1 plasma concentration-time profiles reported in the clinical trials (Supplemental Table 5).

Results

Data Analysis of the Clinical DDI Studies. CYP2B6 in vivo DDI data used for this analysis are presented in Tables 1 and 2. The compiled clinical data contained 14 clinical studies using bupropion as the substrate with seven precipitants, 16 studies using efavirenz as the substrate with nine precipitants, and four precipitants administered with both substrates. In all cases, precipitant and victim drugs were administered orally. In 17 of 30 clinical trials, there was no clinically relevant interaction observed according to the bioequivalence criteria in the FDA DDI guidance (http://www.fda.gov/downloads/drugs/guidancecomplianceregulatoryinformation/guidances/ucm292362) (AUCR = 0.8–1.25). The most pronounced change in AUCR [area under the concentration curve ratio with and without precipitant drug] was mediated by carbamazepine with bupropion as a probe substrate (AUCR = 0.1). Moderate induction was mediated by 4 of 12 precipitants (namely, efavirenz, rifampin, ritonavir, and nevirapine). The magnitude of change observed with rifampin was largely dependent on the efavirenz dosing regimen (a single dose or multiple doses). For ritonavir, a dosage of 600 mg/d for > 1 week caused the most pronounced decrease in the bupropion area under the concentration curve (AUC; up to AUCR = 0.34), and there was a negligible change in efavirenz exposure when 100 mg was administered for 7 days. Similarly, rifampin caused a greater reduction in the bupropion AUC than efavirenz, especially when efavirenz was administered as a single dose (AUCR = 0.44–0.61) versus multiple doses (AUCR = 0.63–0.82).

In Vitro Kinetic Parameter Determination. In vitro induction parameters based on mRNA were generated across multiple companies and data were pooled for each inducer (Table 3; Supplemental Tables 1–4). For compounds in which inhibition was observed, in vitro IC_{50} and K_I/k_{inact} values were also generated. The induction parameters for each inducer were determined from at least two companies and multiple

TABLE 1

Summary of the in vivo bupropion DDI clinical studies used for predictions

Precipitant	Precipitant Dose (Duration)	Precipitant Dose Interval	Bupropion Victim Drug Dose	Bupropion Dose Interval	Observed DDI (AUCR)	Reference
	mg		*mg*			
Carbamazepine	942 (wk)	QD	150	SD	0.10	Ketter et al. (1995)
Cimetidine	800 (1 d)	QD	300	SD	1.05	Kustra et al. (1999)
Efavirenz	600 (15 d)	QD	150	SD	0.45	Robertson et al. (2008)
Nelfinavir	1250 (14 d)	BID	150	SD	0.92	Kirby et al. (2011)
Rifampin	600 (7 d)	QD	150	SD	0.33	Chung et al. (2011)
	600 (10 d)	QD	150	SD	0.33	Loboz et al. (2006)
	600 (10 d)	QD	150	SD	0.52	Kharasch et al. (2008a)
Ritonavir	100 (23 d)	BID	150	SD	0.78	Park et al. (2010)
	200–400 (14 d)	TID	150	SD	0.67	Kirby et al. (2011)
	600 (23 d)	BID	150	SD	0.34	Park et al. (2010)
	200–300 (18 d)	BID	150	SD	0.98	Kharasch et al. (2008b)
	200–300 (3 d)	BID	150	SD	0.84	Kharasch et al. (2008b)
	200 (2 d)	BID	75	SD	1.2	Hesse et al. (2006)
Teriflunomide	14–70 (14 d)	QD	150	SD	0.91	Sheedy et al. (1977)

BID, twice daily; QD, every day; SD, single dose; TID, three times daily.

hepatocyte donors (Supplemental Tables 1–4), and the results are presented as averages. In addition, commonly used in vitro CYP2B6 prototypical inducers such as phenobarbital and phenytoin were included for comparisons with the in vitro profiles determined for the clinical inducer data set.

Inducers that selectively target CYP2B6 were not identified. In contrast, coinduction of CYP3A4 was observed for all tested CYP2B6 inducers. Of note, the EC_{50} values for CYP2B6 induction were lower than CYP3A4 with all compounds except for rifampin. CYP2B6 and CYP3A4 induction parameters for itraconazole and cimetidine could not be determined because of the lack of detectable induction in vitro. CYP3A4 was more sensitive to induction by rifampin (lower EC_{50}, higher E_{max}) than CYP2B6. The EC_{50} and E_{max} ratios for CYP3A4/CYP2B6, E_{max} and EC_{50}, were calculated to evaluate the relative potency of CYP2B6 versus CYP3A4 induction. In all cases, the ratio of CYP3A4/CYP2B6 E_{max} was > 1 (range, 1.4–3.9), confirming that the magnitude of induction mediated for CYP3A4 at the mRNA level is higher than CYP2B6 in vitro (Table 3) and is consistent with previously published data (Faucette et al., 2007; Fahmi et al., 2010). It is worth noting that previously reported data with nevirapine and efavirenz showed higher induction of CYP2B6 than CYP3A4, which may be attributable to the shorter (24-hour) hepatocyte treatment time with test compounds (Faucette et al., 2007). Applying the same comparison with EC_{50} values demonstrated that EC_{50} values between CYP2B6 and CYP3A4 were similar for carbamazepine, indinavir, nelfinavir, and phenobarbital. EC_{50} values were higher for CYP3A4 than CYP2B6 for efavirenz, nevirapine, saquinavir, terifluomide, and phenytoin. Only rifampin had a lower EC_{50} for CYP3A4 than for CYP2B6. Interestingly, the change in enzyme activity for CYP2B6 tended to be similar to the fold increase in mRNA, whereas CYP3A4 mRNA increases were typically higher than corresponding activity (data not shown).

f_m Values for the Clinical Substrates Bupropion and Efavirenz. Initial estimations using the in vitro–derived induction parameters and published IVIVE models for characterizing clinical induction resulted in poor predictions, particularly for bupropion. On the basis of the currently available literature, the lack of IVIVE capability for bupropion was likely attributable to the lack of selectivity of this probe toward CYP2B6. The same data were not available for efavirenz; in addition, there are no strong in vivo inhibition studies to validate the f_m for CYP2B6 toward overall efavirenz metabolism. Therefore, an attempt was made to

TABLE 2

Summary of the in vivo efavirenz DDI clinical studies used for predictions

Precipitant	Precipitant Dose (Duration)	Dose Interval	Efavirenz Victim Drug Dose (Duration)	Efavirenz Dose Interval	Observed DDI (AUCR)	Reference
	mg		*mg*			
Carbamazepine	200–400 (21 d)	QD	600 (35 d)	QD	0.64	Ji et al. (2008)
Ezetimibe	10 (11 d)	QD	400	SD	0.91	Meyer zu Schwabedissen et al. (2012)
	10 (24 d)	QD	400	SD	1.1	Oswald et al. (2012)
Indinavir	1200 (7 d)	BID	600	SD	0.81	Ma et al. (2008)
Itraconazole	200 (6 d)	QD	200	SD	1.0	Jiang et al. (2013)
Nelfinavir	1250 (32 wk)	BID	600 (32 wk)	QD	0.83	Smith et al. (2005)
	1250 (7 d)	BID	600	SD	0.99	Ma et al. (2008)
	750 (>4 wk)	TID	600 (>4 wk)	QD	1.1	Villani et al. (1999)
Nevirapine	400 (4 wk)	QD	600 (6 wk)	QD	0.71	Veldkamp et al. (2001)
Rifampin	450 (7 d)	QD	600	SD	0.61	Yenny et al. (2011)
	600 (10 d)	QD	600	SD	0.44	Cho et al. (2011)
	600 (wk)	QD	600–800 (wk)	QD	0.63[a]	Matteelli et al. (2007)
	10.5 mg/kg (7 d)	QD	600 (14 d)	QD	0.78	López-Cortés et al. (2002)
	600 (8 d)	QD	600 (8 d)	QD	0.82	Kwara et al. (2011)
Ritonavir	100 (7 d)	BID	600	SD	1.0	Ma et al. (2008)
Saquinavir	1600 (7 d)	BID	600	SD	0.89	Ma et al. (2008)

BID, twice daily; CL, clearance; QD, every day; SD, single dose; TID, three times daily.
[a]Observed fold-change in CL ($CL_{control}/CL_{induced}$).

TABLE 3

In vitro determined CYP3A4 and CYP2B6 DDI kinetic parameters

Precipitant	CYP3A4					CYP2B6			Ratio E_{max} CYP3A4/CYP2B6	Ratio EC_{50} CYP3A4/CYP2B6	Ratio E_{max}/EC_{50} CYP3A4/CYP2B6
	K_i	K_I	k_{inact}	E_{max}	EC_{50}	K_i	E_{max}	EC_{50}			
	μM	μM	min^{-1}		μM	μM		μM			
Carbamazepine	100	NA	NA	24.7	43.3	100	14.8	35.4	1.7	1.2	1.4
Cimetidine	100	NA	NA	NA	NA	100	NA	NA	NA	NA	NA
Efavirenz	20.6	NA	NA	19.6	4.59	2.7	10.8	1.62	1.8	2.8	0.64
Ezetimibe	3.3	1.1	0.06	4.90	10.2	5.5	3.48	6.68	1.4	1.5	0.92
Indinavir	0.4	NA	NA	8.30	16.5	40.0	2.29	15.2	3.6	1.1	3.3
Itraconazole	0.10	NA	NA	NA	NA	2.00	NA	NA	NA	NA	NA
Nelfinavir	0.9	2.3	0.10	15	1.51	6.5	4.14	1.43	3.7	1.1	3.4
Nevirapine	100	NA	NA	27	86.3	100	12.2	35.9	2.2	2.4	0.92
Rifampin	100	NA	NA	38	0.66	100	8.26	1.26	4.5	0.5	8.8
Ritonavir	0.004	0.07	0.21	20	1.40	2.3	5.73	0.87	3.5	1.6	2.2
Saquinavir	1.3	7.7	0.09	12	2.82	40.0	3.04	0.63	3.9	4.5	0.88
Teriflunomide	100	NA	NA	4.13	10.3	100	3.03	4.97	1.4	2.1	0.66
Phenobarbital	NA	NA	NA	21.1	347	NA	13.9	347	1.5	1.0	1.5
Phenytoin	NA	NA	NA	25.1	36	NA	14.9	14.3	1.7	2.5	0.67

Ratios of CYP3A4/CYP2B6 are based on the mean values of data generated from various lots. NA, not applicable.

understand the contribution of CYP2B6 in metabolizing efavirenz at its clinically relevant induced steady-state concentration (10 μM) to evaluate the effect of coinduction of CYP2B6 and CYP3A4 on the metabolism through these pathways. The study was designed based on available metabolite identification data and published pathways for clearance of efavirenz.

Efavirenz Metabolism Using the HepatoPac In Vitro Model. A long-term incubation of a human hepatocyte model (HepatoPac) (Ramsden et al., 2015) was used to identify the contribution of CYP2A6, CYP2B6, CYP3A4, and uridine 5′-diphosphoglucuronosyltransferase (UGT; predominately UGT2B7) toward efavirenz metabolism (di Iulio et al., 2009; Kwara et al., 2009; Ogburn et al., 2010; Court et al., 2014) (Table 4). Induced human HepatoPac (with 10 μM ^{14}C-efavirenz) plates were then further incubated with and without inducers for 72 hours (10 μM rifampin, 10 μM efavirenz, or 100 μM carbamazepine) or inhibitors (50 μM erythromycin, 10 μM ticlopidine, 10 μM telmisartan, or 10 μM PCPAH). Where possible, confirmation of metabolite structures was performed using authentic standards and by deconjugation with glucuronidase for the glucuronide conjugates. The metabolic profile was in line with literature reports and the metabolites identified were 8-hydroxy, 8,14-dihydroxy, 8-hydroxyglucuronide, 8,14-dihydroxyglucuronide, 7-hydroxy, 7-hydroxyglucuronide, and efavirenz *N*-glucuronide, whereas 7-hydroxysulfate was not detected.

When human hepatocytes were incubated to the induced state (96- to 120-hour incubation with ^{14}C-efavirenz), the average extent of efavirenz depletion by metabolism across donors was 47% (n = 4), with the primary metabolic route being through the 8-OH pathway (primarily recovered as the glucuronide conjugate), followed by the 7-OH pathway (primarily recovered as the glucuronide conjugate), and lastly through *N*-glucuronidation (as shown in Table 4).

When hepatocytes were treated with [^{14}C]-efavirenz (for up to 120 hours) and allowed to be induced further for 72 hours with either rifampin (10 μM) or carbamazepine (100 μM), only carbamazepine resulted in a pronounced increase in efavirenz depletion by metabolism (approximately 2-fold greater depletion than solvent control) and increased in the 8-OH pathway only, in line with it being an inducer of CYP2B6 and CYP3A4. There was no increase in efavirenz metabolism with the extended rifampin or efavirenz treatment, suggesting that efavirenz autoinduction resulted in the maximal change in CYP2B6/CYP3A4 expression, which is consistent with the clinical observations (Table 2). The difference between carbamazepine and rifampin highlights the overlapping regulation of CYP2B6 and CYP3A4 and their contributions to efavirenz metabolism upon induction. The clinical DDI data showed a difference in magnitude of efavirenz AUCR (with/without rifampin) when multiple efavirenz doses were given (0.63–0.82) versus when a single dose was given (0.44–0.61), as shown in Table 2.

The extent of efavirenz metabolism was decreased in the in vitro study, suggesting a potential inhibitory effect by rifampin or other factors. For example, increased exposure of efavirenz by rifampin was previously observed in clinical studies and was associated in part with

TABLE 4

Efavirenz metabolism using preinduced HepatoPac with ^{14}C-efavirenz

	^{14}C-Efavirenz Percent Change Relative to Solvent Control[a]						
	CYP3A4/CYP2B6 Inducer			CYP2B6 Inhibitor	CYP3A4 Inhibitor	CYP2A6 Inhibitor	*Pan*-UGT Inhibitor
	CBZ	EFV	RIF	TIC	ERY	PCPAH	TEL
8-OH and its glucuronide conjugate	+60	−17	−22	−76	−54	+16	−16
7-OH and its glucuronide conjugate	−26	−33	−37	+88	−22	−94	+48
N-Glucuronide	−60	−37	−60	−59	−54	−79	−98
EFV	−52	+17	+19	+40	+47	+13	+7

Human hepatocytes using HepatoPac cells were initially induced with 10 μM [^{14}C]-efavirenz for 96–120 hours (total radioactivity recovered ranged between 9.7 and 10.4 μM). Induced human HepatoPac plates were then incubated with and without inducers for an additional 72 hours (10 μM RIF, 10 μM EFV, and 100 μM CBZ) or were coincubated with inhibitors (50 μM ERY, 10 μM TIC, 10 μM TEL, and 10 μM PCPAH). CBZ, carbamazepine; EFV, efavirenz; ERY, erythromycin; RIF, rifampin; TEL, telmisartan; TIC, ticlopidine.

[a]Percent change relative to the solvent control is calculated as = 100 − (concentration in presence of inhibitor or inducer/concentration in solvent control × 100). Plus signs indicate an increase in concentration relative to the solvent control and minus signs indicate a decrease in concentration relative to the solvent control.

CYP2B6 polymorphisms (Kwara et al., 2014). Inhibition of CYP2A6 metabolism confirmed that formation of the 7-OH metabolite was mediated predominately by CYP2A6 (94% inhibition of the 7-OH pathway relative to the solvent control). Inhibition of CYP2A6 increased the 8-OH pathway and decreased *N*-glucuronidation.

Inhibition of CYP2B6 metabolism decreased the 8-OH pathway by 76% relative to the solvent control, while increasing the metabolism through the 7-OH pathway from 88% relative to the solvent control, which suggests that this may serve as a compensatory pathway for efavirenz metabolism.

Selective inhibition of CYP3A4 by erythromycin resulted in a decrease in the 8-OH pathway by 54% relative to cells treated with the solvent control. Both the 7-OH pathway and *N*-glucuronidation pathways were increased to 22% and 54% relative to cells treated with the solvent control, respectively. These data confirm that CYP3A4 also plays an important role in the formation of 8-OH efavirenz. When the *pan*-UGT inhibitor telmisartan was added, glucuronidation was significantly inhibited. Formation of efavirenz *N*-glucuronide decreased by 98% relative to cells treated with the solvent control. There was a minimal effect on the 8-OH pathway. However, the 7-OH pathway increased to 48% relative to cells treated with the solvent control, as described in Table 4.

R3 Model. The R3 equation described in the FDA guidance was used for comparison with observed clinical DDI as follows: R3 = $1/(1 + E_{max}[I]/(EC_{50} + [I]))$. The R3 equation uses total (bound + unbound) C_{max} as the inducer input parameter [*I*]. The R3 approach typically represents a conservative estimate of AUCR. Resulting R3 values are displayed in Tables 5 and 6 for bupropion and efavirenz, respectively. Comparing the R3 predictions with the observed AUCR for bupropion and efavirenz resulted in an overprediction of DDIs (Fig. 1). Despite this, there were no false negatives; the percentage of false positives was 44% and 29% for efavirenz and bupropion, respectively.

RIS Model. A correlational approach was used to predict clinical DDIs using RIS calibration curves. The RIS for each precipitant drug was calculated as follows: RIS = $E_{max}[I]/(EC_{50} + [I])$. The RIS equation uses unbound C_{max} as the inducer input parameter [*I*]. This approach uses various inducers with a wide range of induction potencies to generate a correlation curve between in vitro RIS values and observed AUCR changes (Fahmi et al., 2008a). RIS calibration curves were attempted for bupropion (poster presented at the ISSX meeting by Sun et al., 2014) and efavirenz using observed clinical AUCR values. The RIS model with bupropion could not be established, whereas a reasonable correlation ($R^2 = 0.866$) was established with efavirenz (Fig. 2; Tables 5 and 6).

Net Effect Modeling and Comparison with Clinical Outcome. The mechanistic static net effect model described in the EMA and FDA guidance (http://www.ema.europa.eu/docs/en_GB/document_library/Scientific_guideline/2012/07/WC500129606, http://www.fda.gov/downloads/drugs/guidancecomplianceregulatoryinformation/guidances/ucm292362; Fahmi et al., 2008b) was used to predict AUCR for CYP2B6-mediated induction as described in the *Materials and Methods* (Fig. 3). This model incorporates concomitant DDIs such as competitive and time-dependent inhibition along with induction kinetic parameters, in addition to a calculated scalar for in vitro induction data (*d* factor). The f_m CYP2B6 values used in the net effect static model were 0.50 and 0.64 for bupropion and efavirenz, respectively. The magnitude of DDIs could not be accurately predicted with bupropion. Efavirenz resulted in better predicted values ($d = 0.50$) without any observed false negatives or false positives. However, clinical studies using multiple doses of efavirenz were excluded ($n = 3$), owing to the limitation of the net effect model of using one concentration rather than the time-based concentration profile and the inability to account for autoinduction of the probe substrate (Fig. 3; Tables 5 and 6).

PBPK Modeling and Comparison with Clinical Outcome Utilizing SimCYP. A mechanistic dynamic modeling approach was performed using SimCYP. Results are displayed in Tables 5 and 6 and graphically in Fig. 4. The magnitude of DDIs for bupropion tended to be underpredicted using SimCYP. For instance, carbamazepine resulted in a potent clinical interaction (AUCR = 0.1) but the model predicted an AUCR of 0.54 (Table 5). Similarly, efavirenz, ritonavir, and rifampin were clinical inducers (AUCR = 0.44–0.78) but the model predicted an AUCR of 0.79–0.94 (Table 6). The clinical noninducers cimetidine,

TABLE 5

Summary of bupropion DDI predictions

	Dose (Duration)	Predicted DDI (AUCR)			Observed DDI (AUCR)
		R3	Net Effect	SimCYP	AUCR Change
	mg				
Precipitant					
Carbamazepine	942	0.15	0.52	0.54	0.10
Cimetidine	800	0.99	1.0	1.07	1.05
Efavirenz	600	0.09	0.87	0.70	0.45
Nelfinavir	1250	0.21	0.80	0.90	0.92
Rifampin	600	0.12	0.34	0.76	0.33
	600	0.12	0.34	0.68	0.33
	600	0.12	0.34	0.67	0.52
Ritonavir	100	0.20	0.95	0.90	0.78
	400	0.15	0.67	0.79	0.98
	600	0.16	0.75	0.74	0.34
	300	0.16	0.79	0.78	0.67
	300 (3 d)	0.16	0.79	0.89	0.84
	200 (2 d)	0.18	0.90	0.95	1.20
Teriflunomide	14-70	0.94	1.0	0.83	0.91
Prediction error (GMFE)[a]		3.45	1.39	1.50	
True positives		100	75	88	
True negatives		33	67	83	
False positives		67	33	17	
False negatives		0	25	13	

[a]Percentage of clinical trials that were predicted as false negative, false positive, true negative, or true positive with respect to induction based on the 0.8-fold cutoff criterion.

TABLE 6
Summary of efavirenz DDI predictions

	Dose (Duration)	Predicted DDI (AUCR)				Observed DDI (AUCR)
		R3	RIS	Net Effect	SimCYP	AUCR Change
	mg					
Compound						
Carbamazepine	200-400	0.15	0.69	0.64	0.48	0.64
Ezetimibe	10	0.87	0.99	1.00	1.00	0.91
	10	0.87	0.99	1.00	1.00	1.1
Indinavir	200	0.53	0.82	0.93	1.12	0.81
Itraconazole	1250	1.00	1.00	1.00	1.04	1.0
Nelfinavir	750	0.21	0.80	0.87	1.02	0.83
	750	0.21	0.80	0.92	1.02	1.0
	750	0.21	0.80	0.92	1.01	1.1
Nevirapine	400	0.20	0.69	0.65	0.86	0.71
Rifampin	450	0.13	0.66	0.48	0.81	0.61
	600	0.12	0.65	0.44	0.79	0.44
	600	0.12	NA	NA	0.87	0.63
	10.5 mg/kg	0.12	NA	NA	0.94	0.78
	600	0.12	NA	NA	0.92	0.82
Ritonavir	100	0.20	0.94	0.97	0.85	1.0
Saquinavir	1600	0.32	0.93	0.96	1.0	0.89
Prediction error (GMFE)[a]		3.25	1.12	1.09	1.22	
True positives		100	100	100	33	
True negatives		19	100	100	63	
False positives		70	0	0	0	
False negatives		0	0	0	67	

NA, not applicable (data were not included in the prediction, since efavirenz was administered as multiple doses prior to dosing with precipitant drugs).
[a]Percent of clinical trials that were predicted as false negative, false positive, true negative, or true positive with respect to induction based on the 0.8-fold cutoff criterion.

nelfinavir, and teriflunomide were accurately characterized using the mechanistic dynamic modeling approach in SimCYP. There were no false positives observed. However, in one trial, ritonavir resulted in a false positive (AUCR predicted = 0.79; AUCR observed = 0.98). In the case of the mechanistic dynamic model for efavirenz, there were no clinical trials in which potent induction was observed and only 6 of 16 trials had moderate induction results (AUCR = 0.2–0.8). Clinical noninducers ezetimibe, indinavir, and saquinavir were accurately characterized using the mechanistic dynamic modeling approach. The predicted AUCR for carbamazepine (0.48) was slightly lower than the observed AUCR (0.64). Of note, there were five false-negative predictions using this approach (four for rifampin and one for nevirapine).

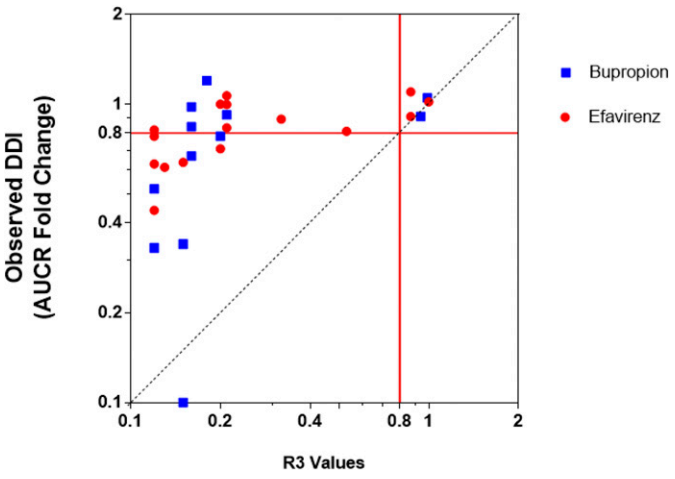

Fig. 1. Basic R3 model–predicted DDIs in which C_{max} is equal to total C_{max}, with efavirenz (circles) and bupropion (squares) as the victim drugs. DDI values are presented as the AUCR fold change.

Discussion

The FDA and EMA DDI guidance documents recommend performing a dedicated clinical CYP2B6 induction study if the new molecular entity (NME) is shown to be a CYP2B6 inducer in vitro, unless the induction potential can be ruled out using predictive mathematical models (http://www.ema.europa.eu/docs/en_GB/document_library/Scientific_guideline/2012/07/WC500129606; http://www.fda.gov/downloads/drugs/guidancecomplianceregulatoryinformation/guidances/ucm292362). These models range from basic static to physiologically based dynamic approaches, with increasing complexity toward the latter. The ability of such models to predict the CYP3A4 induction potential of drugs was previously established (Fahmi et al., 2008a,b; Fahmi and Ripp, 2010; Einolf et al., 2014; Vieira et al., 2014).

In this study, the ability of IVIVE models to predict CYP2B6 induction potential was evaluated. The data presented here suggest that CYP2B6 IVIVE is not possible for the probe substrate bupropion because of the overall significant underprediction of the clinical data, regardless of the mathematical model used (Figs. 1–4; Table 5). A significant scatter and lack of correlation with bupropion using the RIS model suggests a lack of sensitivity perhaps due to the low f_m CYP2B6 for bupropion. When the static or dynamic models were applied, the predicted AUCRs were inconsistent with the observed clinical data, and an overall underprediction was noticed when the observed AUCR values were less than 0.8.

In general, a relatively better IVIVE was achieved for efavirenz compared with bupropion, and there was less misclassification of the inducers according to the cutoff criteria (AUCR = 0.8). With the net effect model, however, a scaling factor (d = 0.50) was applied to efavirenz data to achieve a reasonable correlation without any false negatives (GMFE = 1.09). For efavirenz, PBPK modeling resulted in a reasonable performance in predicting CYP2B6 induction (GMFE = 1.22) (Table 6). However, misclassification leading to false-negative predictions with nevirapine and rifampin was observed.

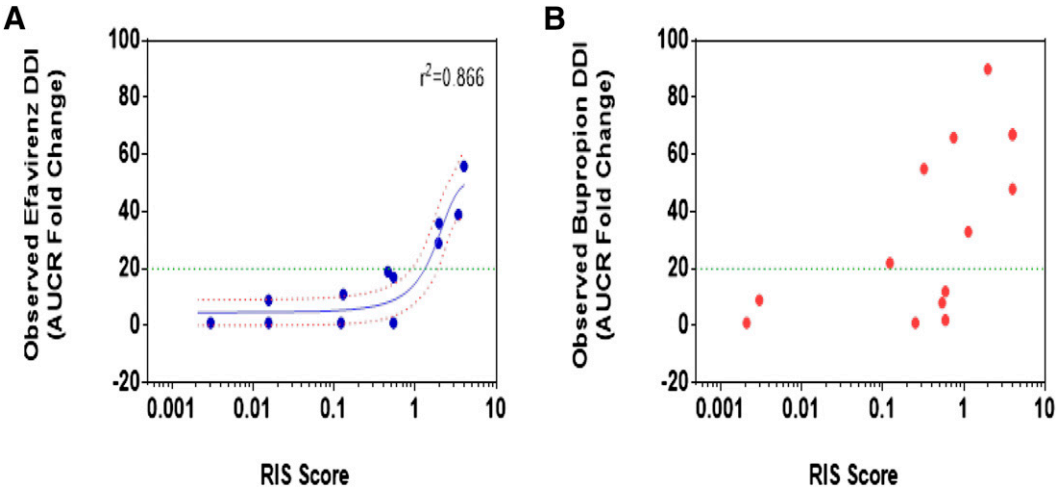

Fig. 2. RIS model–predicted DDIs, with efavirenz (A) and bupropion (B) as the victim drugs. DDI values are presented as the AUCR fold change.

There are several factors that may explain the poor IVIVE for CYP2B6 in this study. One of the major challenges in predicting CYP2B6 induction was the lack of selective, sensitive, and IVIVE validated clinical probe substrates of this enzyme. Although efavirenz and bupropion have been reported to be good probe substrates for CYP2B6 in the literature and in regulatory documents (Walsky et al., 2006), limited data exist to support a high f_m (>0.8) for these two probes. Walsky et al. reported an estimated f_m of 0.9 for efavirenz based on a combination of clinical and in vitro data. However, based on literature information (Faucette et al., 2000; Hesse et al., 2000; Ward et al., 2003; Walsky et al., 2006), the CYP2B6 inhibitor clopidogrel (with an in vitro CYP2B6 IC_{50} = 0.021 μM) was predicted to cause strong inhibition clinically (predicted AUCR = 8.8) if f_m CYP2B6 was assumed to be 0.9. However, clopidogrel clinical DDI data with both bupropion and efavirenz showed minimal interaction (observed AUCR values = 1.36 and 1.26, respectively) (Turpeinen et al., 2005; Jiang et al., 2013), suggesting that efavirenz f_m may not be as high as originally estimated. Recent reports also suggest that bupropion and efavirenz have lower f_m CYP2B6 values of $\leq$ 0.6 (Ke et al., 2016). This low f_m for CYP2B6 clinical probe substrates is also complicated by overlapping metabolism of competing pathways such as CYP3A4, CYP2C19, 11β-hydroxysteroid dehydrogenase, and carbonyl reductase for bupropion (Hesse et al., 2006; Molnari and Myers, 2012; Sage et al., 2015) and CYP3A4, CYP2A6, and UGT2B7 for efavirenz (Ward et al., 2003; Kwara et al., 2011). It was also reported that efavirenz may serve as a better probe substrate for CYP2B6 clinical studies than bupropion when the ratio of 8,14-dihydroxyefavirenz to efavirenz was used as a phenotypic index for CYP2B6 activity in vivo (Jiang et al., 2013).

The autoinduction upon multiple-dose administration of efavirenz results in induction of CYP2B6- and CYP3A4-mediated metabolism. This autoinduction leads to an apparently lower magnitude of DDIs when another inducer is coadministered, compared with when efavirenz is administered as a single dose after the perpetrator. For example, the magnitude of AUCR change was larger for efavirenz when administered as a single dose (Table 2) in the presence of rifampin (AUCR = 0.44–0.61) compared with studies in which both were coadministered for multiple doses (AUCR = 0.63–0.82). This is because comparing steady-state exposures of efavirenz with and without rifampin takes into account autoinduction by efavirenz compared with day 1 when exposure is higher than steady state. As illustrated by the HepatoPac data (Table 4),

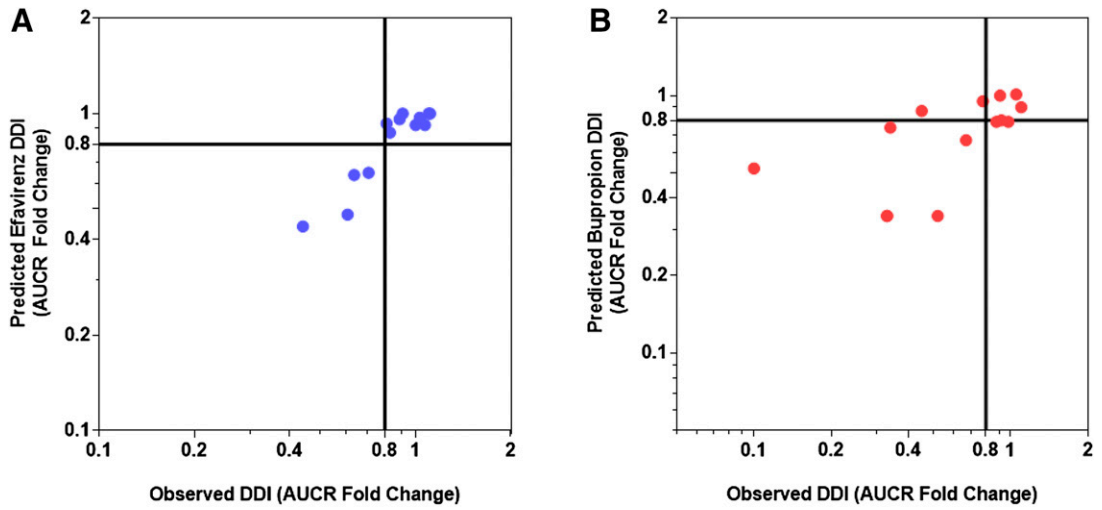

Fig. 3. Net effect model–predicted DDIs compared with observed DDIs, with efavirenz (A) and bupropion (B) as the victim drugs. DDI values are presented as the AUCR fold change.

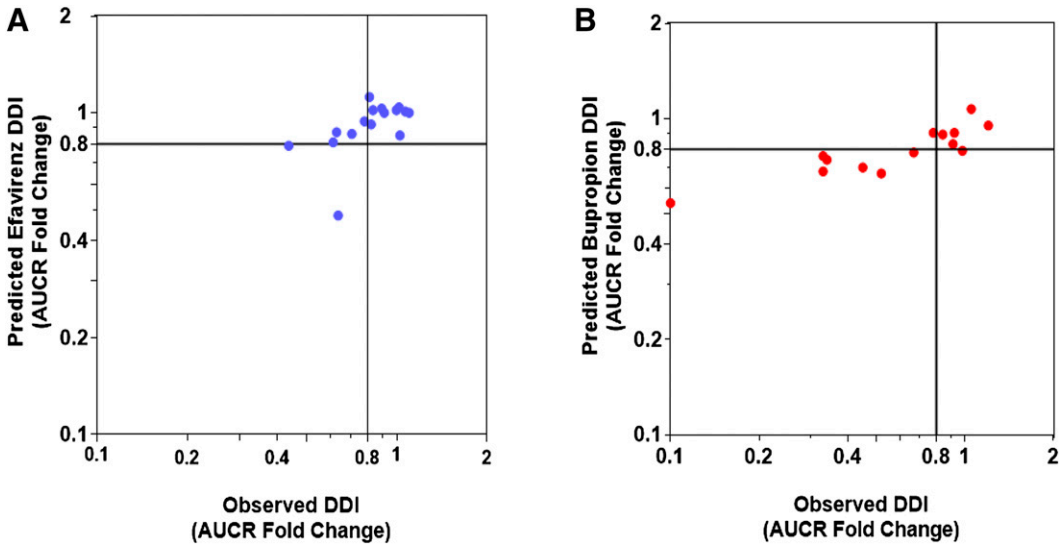

Fig. 4. SimCYP model–predicted DDIs compared with observed DDIs, with efavirenz (A) and bupropion (B) as the victim drugs. DDI values are presented as the AUCR fold change.

the complexity of mimicking the steady state with nonselective marker substrates arises due to coinduction of the CYP3A4 pathway and compensatory pathways that manifest when each pathway is inhibited. The f_m through each pathway is subject to these complex interactions. Therefore, selective marker substrates for CYP2B6 ($f_m > 0.9$) are needed to better model steady-state conditions.

Genetic polymorphisms also play a role in interindividual variability of bupropion (Hesse et al., 2006) and efavirenz pharmacokinetics (Zanger and Klein, 2013) and their responses to inhibitors and inducers (Weerawat et al., 2013). It was also shown that the magnitude of reduction of efavirenz concentrations after multiple dosing was genotype dependent, in which subjects with the CYP2B6*1/*1 genotype (extensive metabolizer) had the largest decrease in their plasma concentrations relative to other CYP2B6 genotypes (Ngaimisi et al., 2010, 2011). This is similar to what was observed previously with CYP2C9 polymorphisms (Lin et al., 2015).

The inducers used in clinical DDI trials (carbamazepine, efavirenz, nevirapine, rifampin, and ritonavir) are not selective inducers for CYP2B6, but they are known to induce both CYP2B6 and CYP3A4 in vitro and in vivo (Fahmi and Ripp, 2010; Fahmi et al., 2010). For example, in vitro data showed that the ratio of CYP3A4 to CYP2B6 maximum induction (E_{max}) was generally higher than unity for all clinical inducers (Table 3), suggesting that CYP3A4 induction may always predominate over CYP2B6. The induction potency of the inducers toward each enzyme as determined by the in vitro EC_{50} values also overlapped between CYP2B6 and CYP3A4 and varied to the same extent across several inducers. For these precipitants, the in vitro observations are supported by the clinical DDI data, in which induction-mediated DDIs with probe substrates of both CYP2B6 and CYP3A4 (Einolf et al., 2014) are reported to be significant (AUCR = 0.65–0.10). To date, selective clinical CYP2B6 inducers have not been identified in vitro or in vivo. Since all of the tested compounds show coinduction of CYP2B6 and CYP3A4, it would be reasonable to question the value of generating CYP2B6 clinical DDI data, especially since confidence in predicting clinical CYP2B6 DDIs is challenged by the lack of selective CYP2B6 inducers and substrates.

In addition, there is a systematic difference in the induction magnitude observed with bupropion versus efavirenz when the same precipitants (rifampin and carbamazepine) were coadministered with each of these substrates. The clinically reported AUCR values (Table 2) were smaller for bupropion (AUCR range, 0.10–0.52) relative to efavirenz (AUCR range, 0.44–0.64), indicating a larger DDI with bupropion as a victim drug with these inducers. The stronger DDI with bupropion could be rationalized by the coinduction of CYP3A4 and CYP2B6 and a relatively larger contribution of CYP3A4 to its metabolism compared with efavirenz.

There are relatively few pharmaceuticals in which CYP2B6 is the major contributor to total clearance (Turpeinen and Zanger, 2012). The clinical data set used for this analysis contained multiple examples where competing inhibition could mask the potential induction of CYP3A4 if used as a surrogate perpetrator for CYP2B6 induction (itraconazole, nelfinavir, ritonavir, and saquinavir).

Given the current limitations in establishing IVIVE for CYP2B6 induction, alternative strategies may be applied as follows. For NMEs that exhibit CYP2B6 and CYP3A4 induction in vitro, a clinical CYP3A4 DDI study could serve as a surrogate for identifying the potential risk for CYP2B6 induction in the clinic (unless confounded by TDI), since induction with sensitive CYP3A4 substrates with all known clinical CYP3A4 inducers (described in this article) results in changes in AUC that are much greater than those for bupropion and efavirenz. Practically, after generating in vitro EC_{50} and E_{max} values for CYP2B6 and CYP3A4 utilizing hepatocytes from three donors, modeling of CYP3A4 in vitro data using established IVIVE methods would determine whether clinical induction assessment for CYP3A4 is necessary. If induction of CYP3A4 is predicted and clinical induction is observed with a sensitive clinical probe substrate (i.e., midazolam), validation of the CYP3A4 IVIVE model can be performed and used to leverage the CYP2B6 in vitro induction data to perform a clinical risk assessment for CYP2B6 [i.e., calibration based on the in vitro E_{max} ratio (CYP3A4/CYP2B6) to estimate a scaling factor]. If the CYP3A4 clinical induction study is negative or mild, it can be concluded that the likelihood of CYP2B6 clinical induction is low and a clinical study for CYP2B6 may not be warranted. For an NME for which CYP3A4 inhibition (reversible or TDI) is observed in vitro along with induction, the potential for CYP2B6 induction may need an independent investigation.

The potential need for a clinical assessment of CYP2B6 induction may depend on other factors, such as the concomitant administration of

CYP2B6 substrates in the targeted patient population or nonchronic treatment duration and regimens for the NME. If a more selective CYP2B6 clinical probe would be identified or if CYP2B6 in vitro induction is observed in the absence of CYP3A4 induction, an investigation of CYP2B6 induction clinically with a dedicated DDI study could prove useful using single-dose efavirenz as a substrate.

Overall, this study highlights the challenges in using current IVIVE approaches for evaluating CYP2B6 induction potential of NMEs, and it proposes alternative strategies to assess DDI risk on a case-by-case basis.

Acknowledgments

The authors thank Georgy Hartman and Pramila Kumari (Merck Research Laboratories); Lai Wang and Dung Yu Chun (Novartis); Philip Clark and Dung Nguyen (GlaxoSmithKline); Ming Zheng (Bristol-Myers Squibb); Anitha Saravanakumar, Jian Lin, Kelly Nulick, Zhiwu Lin, Nat Johnson, Xin Yang, and Kimberly Lapham (Pfizer Inc.); and Jun Sun (AbbVie Inc.) for generating in vitro data, collating in vivo data, and/or contributing to the SimCYP analysis. The authors also thank reviewers from IQ DMLG and Lei Zhang, Ping Zhao, and Shiew-Mei Huang (FDA) for valuable discussions. The views expressed in this article are those of the authors and do not necessarily reflect official views of the EMA or FDA.

Authorship Contributions

Participated in research design: Fahmi, Shebley, Palamanda, Sinz, Ramsden, Einolf, Chen, Wang.

Conducted experiments: Fahmi, Shebley, Palamanda, Sinz, Ramsden, Einolf, Chen, Wang.

Contributed new reagents or analytic tools: Fahmi, Shebley, Palamanda, Sinz, Ramsden, Einolf, Chen, Wang.

Performed data analysis: Fahmi, Shebley, Palamanda, Sinz, Ramsden, Einolf, Chen, Wang.

Wrote or contributed to the writing of the manuscript: Fahmi, Shebley, Palamanda, Sinz, Ramsden, Einolf, Chen, Wang.

References

Bjornsson TD, Callaghan JT, Einolf HJ, Fischer V, Gan L, Grimm S, Kao J, King SP, Miwa G, Ni L, et al.; Pharmaceutical Research and Manufacturers of America (PhRMA) Drug Metabolism/Clinical Pharmacology Technical Working Group; ; FDA Center for Drug Evaluation and Research (CDER) (2003) The conduct of in vitro and in vivo drug-drug interaction studies: a Pharmaceutical Research and Manufacturers of America (PhRMA) perspective. *Drug Metab Dispos* **31**:815–832.

Cho DY, Ogburn ET, Jones D, and Desta Z (2011) Contribution of N-glucuronidation to efavirenz elimination in vivo in the basal and rifampin-induced metabolism of efavirenz. *Antimicrob Agents Chemother* **55**:1504–1509.

Chung JY, Cho JY, Lim HS, Kim JR, Yu KS, Lim KS, Shin SG, and Jang IJ (2011) Effects of pregnane X receptor (NR1I2) and CYP2B6 genetic polymorphisms on the induction of bupropion hydroxylation by rifampin. *Drug Metab Dispos* **39**:92–97.

Court MH, Almutairi FE, Greenblatt DJ, Hazarika S, Sheng H, Klein K, Zanger UM, Bourgea J, Patten CJ, and Kwara A (2014) Isoniazid mediates the CYP2B6*6 genotype-dependent interaction between efavirenz and antituberculosis drug therapy through mechanism-based inactivation of CYP2A6. *Antimicrob Agents Chemother* **58**:4145–4152.

Court MH, Duan SX, Hesse LM, Venkatakrishnan K, and Greenblatt DJ (2001) Cytochrome P-450 2B6 is responsible for interindividual variability of propofol hydroxylation by human liver microsomes. *Anesthesiology* **94**:110–119.

di Iulio J, Fayet A, Arab-Alameddine M, Rotger M, Lubomirov R, Cavassini M, Furrer H, Günthard HF, Colombo S, Csajka C, et al.; Swiss HIV Cohort Study (2009) In vivo analysis of efavirenz metabolism in individuals with impaired CYP2A6 function. *Pharmacogenet Genomics* **19**:300–309.

Einolf HJ, Chen L, Fahmi OA, Gibson CR, Obach RS, Shebley M, Silva J, Sinz MW, Unadkat JD, Zhang L, et al. (2014) Evaluation of various static and dynamic modeling methods to predict clinical CYP3A induction using in vitro CYP3A4 mRNA induction data. *Clin Pharmacol Ther* **95**:179–188.

Ekins S, Vandenbranden M, Ring BJ, Gillespie JS, Yang TJ, Gelboin HV, and Wrighton SA (1998) Further characterization of the expression in liver and catalytic activity of CYP2B6. *J Pharmacol Exp Ther* **286**:1253–1259.

Fahmi OA, Boldt S, Kish M, Obach RS, and Tremaine LM (2008a) Prediction of drug-drug interactions from in vitro induction data: application of the relative induction score approach using cryopreserved human hepatocytes. *Drug Metab Dispos* **36**:1971–1974.

Fahmi OA, Hurst S, Plowchalk D, Cook J, Guo F, Youdim K, Dickins M, Phipps A, Darekar A, Hyland R, et al. (2009) Comparison of different algorithms for predicting clinical drug-drug interactions, based on the use of CYP3A4 in vitro data: predictions of compounds as precipitants of interaction. *Drug Metab Dispos* **37**:1658–1666.

Fahmi OA, Kish M, Boldt S, and Obach RS (2010) Cytochrome P450 3A4 mRNA is a more reliable marker than CYP3A4 activity for detecting pregnane X receptor-activated induction of drug-metabolizing enzymes. *Drug Metab Dispos* **38**:1605–1611.

Fahmi OA, Maurer TS, Kish M, Cardenas E, Boldt S, and Nettleton D (2008b) A combined model for predicting CYP3A4 clinical net drug-drug interaction based on CYP3A4 inhibition, inactivation, and induction determined in vitro. *Drug Metab Dispos* **36**:1698–1708.

Fahmi OA and Ripp SL (2010) Evaluation of models for predicting drug-drug interactions due to induction. *Expert Opin Drug Metab Toxicol* **6**:1399–1416.

Faucette SR, Hawke RL, Lecluyse EL, Shord SS, Yan B, Laethem RM, and Lindley CM (2000) Validation of bupropion hydroxylation as a selective marker of human cytochrome P450 2B6 catalytic activity. *Drug Metab Dispos* **28**:1222–1230.

Faucette SR, Zhang TC, Moore R, Sueyoshi T, Omiecinski CJ, LeCluyse EL, Negishi M, and Wang H (2007) Relative activation of human pregnane X receptor versus constitutive androstane receptor defines distinct classes of CYP2B6 and CYP3A4 inducers. *J Pharmacol Exp Ther* **320**:72–80.

Hesse LM, Greenblatt DJ, von Moltke LL, and Court MH (2006) Ritonavir has minimal impact on the pharmacokinetic disposition of a single dose of bupropion administered to human volunteers. *J Clin Pharmacol* **46**:567–576.

Hesse LM, Venkatakrishnan K, Court MH, von Moltke LL, Duan SX, Shader RI, and Greenblatt DJ (2000) CYP2B6 mediates the in vitro hydroxylation of bupropion: potential drug interactions with other antidepressants. *Drug Metab Dispos* **28**:1176–1183.

Hidestrand M, Oscarson M, Salonen JS, Nyman L, Pelkonen O, Turpeinen M, and Ingelman-Sundberg M (2001) CYP2B6 and CYP2C19 as the major enzymes responsible for the metabolism of selegiline, a drug used in the treatment of Parkinson's disease, as revealed from experiments with recombinant enzymes. *Drug Metab Dispos* **29**:1480–1484.

Ji P, Damle B, Xie J, Unger SE, Grasela DM, and Kaul S (2008) Pharmacokinetic interaction between efavirenz and carbamazepine after multiple-dose administration in healthy subjects. *J Clin Pharmacol* **48**:948–956.

Jiang F, Desta Z, Shon JH, Yeo CW, Kim HS, Liu KH, Bae SK, Lee SS, Flockhart DA, and Shin JG (2013) Effects of clopidogrel and itraconazole on the disposition of efavirenz and its hydroxyl metabolites: exploration of a novel CYP2B6 phenotyping index. *Br J Clin Pharmacol* **75**:244–253.

Ke A, Barter Z, Yeo K, and Almond L (2016) Toward a best practice approach in PBPK modeling: case example of developing a unified efavirenz model accounting for induction of CYPs 3A4 and 2B6. *CPT Pharmacometrics Syst Pharmacol* DOI: 10.1002/psp4.12088 [published ahead of print].

Ketter TA, Jenkins JB, Schroeder DH, Pazzaglia PJ, Marangell LB, George MS, Callahan AM, Hinton ML, Chao J, and Post RM (1995) Carbamazepine but not valproate induces bupropion metabolism. *J Clin Psychopharmacol* **15**:327–333.

Kharasch ED, Mitchell D, and Coles R (2008a) Stereoselective bupropion hydroxylation as an in vivo phenotypic probe for cytochrome P4502B6 (CYP2B6) activity. *J Clin Pharmacol* **48**:464–474.

Kharasch ED, Mitchell D, Coles R, and Blanco R (2008b) Rapid clinical induction of hepatic cytochrome P4502B6 activity by ritonavir. *Antimicrob Agents Chemother* **52**:1663–1669.

Kirby BJ, Collier AC, Kharasch ED, Dixit V, Desai P, Whittington D, Thummel KE, and Unadkat JD (2011) Complex drug interactions of HIV protease inhibitors 2: in vivo induction and in vitro to in vivo correlation of induction of cytochrome P450 1A2, 2B6, and 2C9 by ritonavir or nelfinavir. *Drug Metab Dispos* **39**:2329–2337.

Kustra R, Corrigan B, Dunn J, Duncan B, and Hsyu PH (1999) Lack of effect of cimetidine on the pharmacokinetics of sustained-release bupropion. *J Clin Pharmacol* **39**:1184–1188.

Kwara A, Cao L, Yang H, Poethke P, Kurpewski J, Tashima KT, Mahjoub BD, Court MH, and Peloquin CA (2014) Factors associated with variability in rifampin plasma pharmacokinetics and the relationship between rifampin concentrations and induction of efavirenz clearance. *Pharmacotherapy* **34**:265–271.

Kwara A, Lartey M, Sagoe KW, Kenu E, and Court MH (2009) CYP2B6, CYP2A6 and UGT2B7 genetic polymorphisms are predictors of efavirenz mid-dose concentration in HIV-infected patients. *AIDS* **23**:2101–2106.

Kwara A, Tashima KT, Dumond JB, Poethke P, Kurpewski J, Kashuba AD, Court MH, and Greenblatt DJ (2011) Modest but variable effect of rifampin on steady-state plasma pharmacokinetics of efavirenz in healthy African-American and Caucasian volunteers. *Antimicrob Agents Chemother* **55**:3527–3533.

Lehmann JM, McKee DD, Watson MA, Willson TM, Moore JT, and Kliewer SA (1998) The human orphan nuclear receptor PXR is activated by compounds that regulate CYP3A4 gene expression and cause drug interactions. *J Clin Invest* **102**:1016–1023.

Lin J, Zhang Y, Zhou H, Wang X, and Wang W (2015) CYP2C9 genetic polymorphism is a potential predictive marker for the efficacy of rosuvastatin therapy. *Clin Lab* **61**:1317–1324.

Loboz KK, Gross AS, Williams KM, Liauw WS, Day RO, Blievernicht JK, Zanger UM, and McLachlan AJ (2006) Cytochrome P450 2B6 activity as measured by bupropion hydroxylation: effect of induction by rifampin and ethnicity. *Clin Pharmacol Ther* **80**:75–84.

López-Cortés LF, Ruiz-Valderas R, Viciana P, Alarcón-González A, Gómez-Mateos J, León-Jimenez E, Sarasanacenta M, López-Pua Y, and Pachón J (2002) Pharmacokinetic interactions between efavirenz and rifampicin in HIV-infected patients with tuberculosis. *Clin Pharmacokinet* **41**:681–690.

Ma Q, Forrest A, Rosenkranz SL, Para MF, Yarasheski KE, Reichman RC, and Morse GD; ACTG A5043 Protocol Team, DAIDS, NIH (2008) Pharmacokinetic interaction between efavirenz and dual protease inhibitors in healthy volunteers. *Biopharm Drug Dispos* **29**:91–101.

Matteelli A, Regazzi M, Villani P, De Iaco G, Cusato M, Carvalho AC, Caligaris S, Tomasoni L, Manfrin M, Capone S, et al. (2007) Multiple-dose pharmacokinetics of efavirenz with and without the use of rifampicin in HIV-positive patients. *Curr HIV Res* **5**:349–353.

Meyer zu Schwabedissen HE, Oswald S, Bresser C, Nassif A, Modess C, Desta Z, Ogburn ET, Marinova M, Lütjohann D, Spielhagen C, et al. (2012) Compartment-specific gene regulation of the CAR inducer efavirenz in vivo. *Clin Pharmacol Ther* **92**:103–111.

Molnari JC and Myers AL (2012) Carbonyl reduction of bupropion in human liver. *Xenobiotica* **42**:550–561.

Ngaimisi E, Mugusi S, Minzi O, Sasi P, Riedel KD, Suda A, Ueda N, Janabi M, Mugusi F, Haefeli WE, et al. (2011) Effect of rifampicin and CYP2B6 genotype on long-term efavirenz autoinduction and plasma exposure in HIV patients with or without tuberculosis. *Clin Pharmacol Ther* **90**:406–413.

Ngaimisi E, Mugusi S, Minzi OM, Sasi P, Riedel KD, Suda A, Ueda N, Janabi M, Mugusi F, Haefeli WE, et al. (2010) Long-term efavirenz autoinduction and its effect on plasma exposure in HIV patients. *Clin Pharmacol Ther* **88**:676–684.

Ogburn ET, Jones DR, Masters AR, Xu C, Guo Y, and Desta Z (2010) Efavirenz primary and secondary metabolism in vitro and in vivo: identification of novel metabolic pathways and cytochrome P450 2A6 as the principal catalyst of efavirenz 7-hydroxylation. *Drug Metab Dispos* **38**:1218–1229.

Oswald S, Meyer zu Schwabedissen HE, Nassif A, Modess C, Desta Z, Ogburn ET, Mostertz J, Keiser M, Jia J, Hubeny A, et al. (2012) Impact of efavirenz on intestinal metabolism and transport: insights from an interaction study with ezetimibe in healthy volunteers. *Clin Pharmacol Ther* **91**:506–513.

Park J, Vousden M, Brittain C, McConn DJ, Iavarone L, Ascher J, Sutherland SM, and Muir KT (2010) Dose-related reduction in bupropion plasma concentrations by ritonavir. *J Clin Pharmacol* **50**:1180–1187.

Ramsden D, Zhou J, and Tweedie DJ (2015) Determination of a degradation constant for CYP3A4 by direct suppression of mRNA in a novel human hepatocyte model, HepatoPac. *Drug Metab Dispos* **43**:1307–1315.

Robertson SM, Maldarelli F, Natarajan V, Formentini E, Alfaro RM, and Penzak SR (2008) Efavirenz induces CYP2B6-mediated hydroxylation of bupropion in healthy subjects. *J Acquir Immune Defic Syndr* **49**:513–519.

Roy P, Yu LJ, Crespi CL, and Waxman DJ (1999) Development of a substrate-activity based approach to identify the major human liver P-450 catalysts of cyclophosphamide and ifosfamide activation based on cDNA-expressed activities and liver microsomal P-450 profiles. *Drug Metab Dispos* **27**:655–666.

Sage JS, Le H, Chang J, and Isoherrane N (2015) New metabolic pathways of bupropion in vivo reveal an important role of CYP2C19 and 11B-HSD in bupropion clearance; CYP2B6 contribution to bupropion clearance is minor. *ACS Med Chem Lett* DOI: 10.1021/acsmedchemlett.6b00189 [published ahead of print].

Sheedy PF, 2nd, Stephens DH, Hattery RR, MacCarty RL, and Williamson B, Jr (1977) Computed tomography of the pancreas. *Radiol Clin North Am* **15**:349–366.

Smith PF, Robbins GK, Shafer RW, Wu H, Yu S, Hirsch MS, Merigan TC, Park JG, Forrest A, Fischl MA, et al.; ACTG 384-5006 Team (2005) Pharmacokinetics of nelfinavir and efavirenz in antiretroviral-naive, human immunodeficiency virus-infected subjects when administered alone or in combination with nucleoside analog reverse transcriptase inhibitors. *Antimicrob Agents Chemother* **49**:3558–3561.

Sueyoshi T, Kawamoto T, Zelko I, Honkakoski P, and Negishi M (1999) The repressed nuclear receptor CAR responds to phenobarbital in activating the human CYP2B6 gene. *J Biol Chem* **274**:6043–6046.

Tolson AH and Wang H (2010) Regulation of drug-metabolizing enzymes by xenobiotic receptors: PXR and CAR. *Adv Drug Deliv Rev* **62**:1238–1249.

Turpeinen M, Tolonen A, Uusitalo J, Jalonen J, Pelkonen O, and Laine K (2005) Effect of clopidogrel and ticlopidine on cytochrome P450 2B6 activity as measured by bupropion hydroxylation. *Clin Pharmacol Ther* **77**:553–559.

Turpeinen M and Zanger UM (2012) Cytochrome P450 2B6: function, genetics, and clinical relevance. *Drug Metabol Drug Interact* **27**:185–197.

Veldkamp AI, Harris M, Montaner JS, Moyle G, Gazzard B, Youle M, Johnson M, Kwakkelstein MO, Carlier H, van Leeuwen R, et al. (2001) The steady-state pharmacokinetics of efavirenz and nevirapine when used in combination in human immunodeficiency virus type 1-infected persons. *J Infect Dis* **184**:37–42.

Vieira ML, Kirby B, Ragueneau-Majlessi I, Galetin A, Chien JY, Einolf HJ, Fahmi OA, Fischer V, Fretland A, Grime K, et al. (2014) Evaluation of various static in vitro-in vivo extrapolation models for risk assessment of the CYP3A inhibition potential of an investigational drug. *Clin Pharmacol Ther* **95**:189–198.

Villani P, Regazzi MB, Castelli F, Viale P, Torti C, Seminari E, and Maserati R (1999) Pharmacokinetics of efavirenz (EFV) alone and in combination therapy with nelfinavir (NFV) in HIV-1 infected patients. *Br J Clin Pharmacol* **48**:712–715.

Walsky RL, Astuccio AV, and Obach RS (2006) Evaluation of 227 drugs for in vitro inhibition of cytochrome P450 2B6. *J Clin Pharmacol* **46**:1426–1438.

Wang H and Tompkins LM (2008) CYP2B6: new insights into a historically overlooked cytochrome P450 isozyme. *Curr Drug Metab* **9**:598–610.

Ward BA, Gorski JC, Jones DR, Hall SD, Flockhart DA, and Desta Z (2003) The cytochrome P450 2B6 (CYP2B6) is the main catalyst of efavirenz primary and secondary metabolism: implication for HIV/AIDS therapy and utility of efavirenz as a substrate marker of CYP2B6 catalytic activity. *J Pharmacol Exp Ther* **306**:287–300.

Weerawat W, Pichitlamken J, and Subsombat P (2013) A generic discrete-event simulation model for outpatient clinics in a large public hospital. *J Healthc Eng* **4**:285–305.

Xie W, Barwick JL, Simon CM, Pierce AM, Safe S, Blumberg B, Guzelian PS, and Evans RM (2000) Reciprocal activation of xenobiotic response genes by nuclear receptors SXR/PXR and CAR. *Genes Dev* **14**:3014–3023.

Yenny N, Nafrialdi, Djoerban Z, and Setiabudy R (2011) Pharmacokinetic interaction between efavirenz and rifampicin in healthy volunteers. *Int J Clin Pharmacol Ther* **49**:162–168.

Zanger UM and Klein K (2013) Pharmacogenetics of cytochrome P450 2B6 (CYP2B6): advances on polymorphisms, mechanisms, and clinical relevance. *Front Genet* **4**:24.

Zanger UM, Klein K, Saussele T, Blievernicht J, Hofmann MH, and Schwab M (2007) Polymorphic CYP2B6: molecular mechanisms and emerging clinical significance. *Pharmacogenomics* **8**:743–759.

Address correspondence to: Dr. Odette A. Fahmi, Department of Pharmacokinetics, Dynamics, and Metabolism, Pfizer Inc., Eastern Point Road, Groton, CT 06340. E-mail: odette.a.fahmi@pfizer.com